

Effect of Citric Acid on the Synthesis of MoP Catalyst for CO₂ Reforming of CH₄

^{1,2}Hui-Rui Guo, ¹Xian-Cai Li*, ¹Ai-Jun Yang, ¹Yi-Feng Yang and ¹Li-Li Yu

¹College of Chemistry, Nanchang University, Nanchang 330031, Jiangxi, China.

²College of Chemistry and Biology engineering, Yichun University, Yichun 336000, Jiangxi, China.

xcli@ncu.edu.cn*

(Received on 26th December 2015, accepted in revised form 22nd January 2016)

Summary: A new molybdenum phosphide (MoP) catalyst was successfully synthesized for CO₂ reforming of CH₄ reaction. The catalysts were prepared by temperature-programmed reduction (TPR) of phosphomolybdate precursors which were modified by citric acid (CA) at the molar ratio of MoP:CA = 1: x (x = 0, 1.0, 2.0, 3.0), which were characterized by means of X-ray diffraction (XRD), N₂ adsorption-desorption and CO₂-TPD techniques. The results showed that the addition of citric acid can affect the catalytic activity and that the MoP catalyst had the highest catalytic activity at 1073 K and X=1. After reduced in H₂ flow at 923 K, the activity of the post-reaction catalyst can be well restored, while its structure remains unchanged. In higher temperatures, the samples exhibit good anti-sintering ability and stability.

Keywords: Molybdenum Phosphide; Citric acid; Reforming; Catalysts; CO₂; CH₄.

Introduction

Recently, the dry reforming of methane with carbon dioxide (DRM) has attracted increasing research attention as the reaction can produce a gas mixture of H₂/CO with the molar ratio close to 1. The syngas with such ratio is suitable feedstock for the Fischer–Tropsch synthesis of clean liquid fuels or for some specific fuel cells [1]. Furthermore, CH₄ and CO₂ are greenhouse effect gasses, and are under intense scientific scrutiny for the environment impact and energy resource management [2]. So far, the conventional studies on catalysts towards DRM process have been focused on two different types: noble and non-noble metals. Noble metals have good catalytic activities and resistance to carbon deposition [3, 4], but the prices are very high for large scale implementations. Non-noble metals such as Ni, Fe, Co, Mn and Cu have reasonably good catalytic activities and low prices, but carbon deposit is a serious limitation to catalyst activities. It is hence highly desirable to research new catalyst that is active, stable and cheap for the DRM reaction. Different approaches have been researched to solve such problem [5-9], including metal additives, carrier and coking formation. There is a steady research interest in doping the non-noble metal catalysts with trace amounts of noble metals for the development of composite catalysts [10]. Despite all these attempts, the main problems have not been satisfactorily solved yet.

Transition metal phosphides have been much noted for their outstanding catalytic activity

and stability at hydrodesulfurization (HDS) and hydrodenitrogenation (HDN) reactions [11]. Recently, many transition metal phosphides have been produced by the direct reduction of phosphate at relatively low temperatures [12-15]. Oxides (Al₂O₃, SiO₂) supported MoP catalyst have been applied as a substitute for MoS₂ catalyst in HDS and HDN reactions [16, 17]. Until now there has been no report on the use of MoP as a catalyst for the DRM reaction. In this paper, catalytic activity of MoP catalysts prepared with different CA/MoP molar ratio has been described.

Experimental

Catalysts Preparation

The procedure used for sample preparation was adopted from that by T. Zhang [18]. Stoichiometric amount of CA (*x* is defined as the molar ratio of CA/MoP, *x* = 0, 1, 2, 3) was added into a mixed aqueous solution of (NH₄)₆Mo₇O₂₄·4H₂O and (NH₄)₂HPO₄, aged at 353 K for 12 hours, dried at 393K overnight, and then calcined at 773 K for 5 hours. The oxide precursor was pelletized and sieved to 60/80 mesh, then reduced to phosphide by temperature programmed reduction in flowing H₂ at 923K for 2h (heating to 623 K in 0.5 h, then to 923K at a heating rate of 1 K/min). After being cooled to room temperature in Ar, the sample was passivated under a flow of 1.0 vol% O₂/Ar for 4 h. This resulting catalyst was denoted as MoP-CA_{*x*}.

*To whom all correspondence should be addressed.

Catalytic Activity Tests

Catalytic activities were tested in a fixed-bed micro-reactor. 0.15 g of catalyst was loaded into a U-tube with inner diameter of 4 mm, which was reduced in situ by 60 ml/min flowing H₂ at 923K for 1h. The pulse experiment was carried out in the reactor under the following conditions: feed molar ratio of CH₄/CO₂=1, 0.1MPa, GHSV=1.2×10⁴ ml·(g·h)⁻¹ and argon was used as carrier gas. Product gases were analyzed online by a gas chromatography (GC 102M) equipped with a thermal conductivity detector (TCD) and a Carbosiever SII column for the gas composition analysis.

Catalysts Characterization

N₂ adsorption-desorption isotherms for MoP-CA_x samples were measured at 77 K using a Micromeritics ASAP 2020 instrument. Before the experiments, the samples were degassed at 523 K for 5 h under vacuum. The specific surface area (S_{BET}) was calculated from the N₂ adsorption isotherm using five-point BET method with a value of 0.162 nm² for the cross-sectional area of a N₂ molecule.

Powder X-ray diffraction (XRD) measurements were obtained with a Rigaku D/max-2500 diffractometer using Cu K α radiation ($\lambda=1.54056\text{\AA}$). The analysis conditions were as follows: tube voltage 40 kV; tube current 40 mA; scan speed 4°/min; scan range 10–80°. The phase identification was referenced to standard diffraction file (JCPDS24-0771).

Temperature-programmed desorption (TPD) experiments were carried out in an integrated apparatus including a gas chromatograph and a data processing system. The loaded catalyst was 0.10 g. The loaded catalyst was firstly reduced with H₂ (60 ml/min) at 923 K for 2 hours and then cooled to room temperature under Argon flow (30 ml/min). Subsequently, the catalyst was saturated with CO₂ adsorption gas until dynamic equilibrium, and then flushed with Argon until the base line of the integrator was stabilized. TPD measurement was immediately started at a temperature ramp rate of 10 K/min to a final temperature of 900 K.

Results and Discussion

Effects of CA Addition on the Structure of Molybdenum Phosphide Catalysts

Table-1 lists the textural properties of different MoP-CA_x samples reduced at 923K. The MoP-CA₀ sample prepared by the conventional method had a relatively small surface area of 8.0 m²/g, which was close to that reported by Oyama [13]. With the addition of CA, the surface areas increased greatly. For example, the surface areas of MoP-CA₁, MoP-CA₂ and MoP-CA₃ were 26.1, 87.3 and 22.3 m²·g⁻¹, respectively. This was attributed to the promoting effect of CA. Firstly, Mo⁶⁺ ion likely formed a complex with CA and thus prevented the aggregation of the ions, which facilitated the formation of smaller catalyst particles with increased porosity. In addition, sample prepared with CA would generate large amounts of gas during the calcination, which facilitated the formation of sample with high porosity and large specific surface area. Fig. 1 shows the typical N₂ adsorption-desorption isotherms for MoP-CA_x samples. With the increase in the amount of CA, the capacities of N₂ adsorption also increased. A long range hysteresis loop at P/P₀ with values from 0.4 to 1.0 occurred for MoP-CA₁. For MoP-CA₂, the hysteresis loops shifted to P/P₀ values at 0.4–0.6 with an increase in the total volume adsorbed, suggesting the existence of ink-bottle type mesopores. The hysteresis loops disappeared when the CA/Mo molar ratio was 3. More CA could be aggregated as template and further formed as macropores during the MoP formation. Thus, with the increase of *x*, the pores in the samples transformed from micropore to mesopore, and to the pores formed by the cluster of the MoP particles [18].

Table-1: Textural properties of different MoP samples.

Sample	S_{BET} (m ² ·g ⁻¹)	Pore volume (cm ³ ·g ⁻¹)	Pore diameter (nm)	Crystallite size (nm) ^a
MoP-CA ₀	8.0	0.041	20.5	18.2
MoP-CA ₁	26.1	0.046	7.1	9.4
MoP-CA ₂	87.3	0.078	3.6	8.6
MoP-CA ₃	22.3	0.082	14.7	9.9

^a calculated from the X-ray diffraction patterns for these samples by the Sherrer equation.

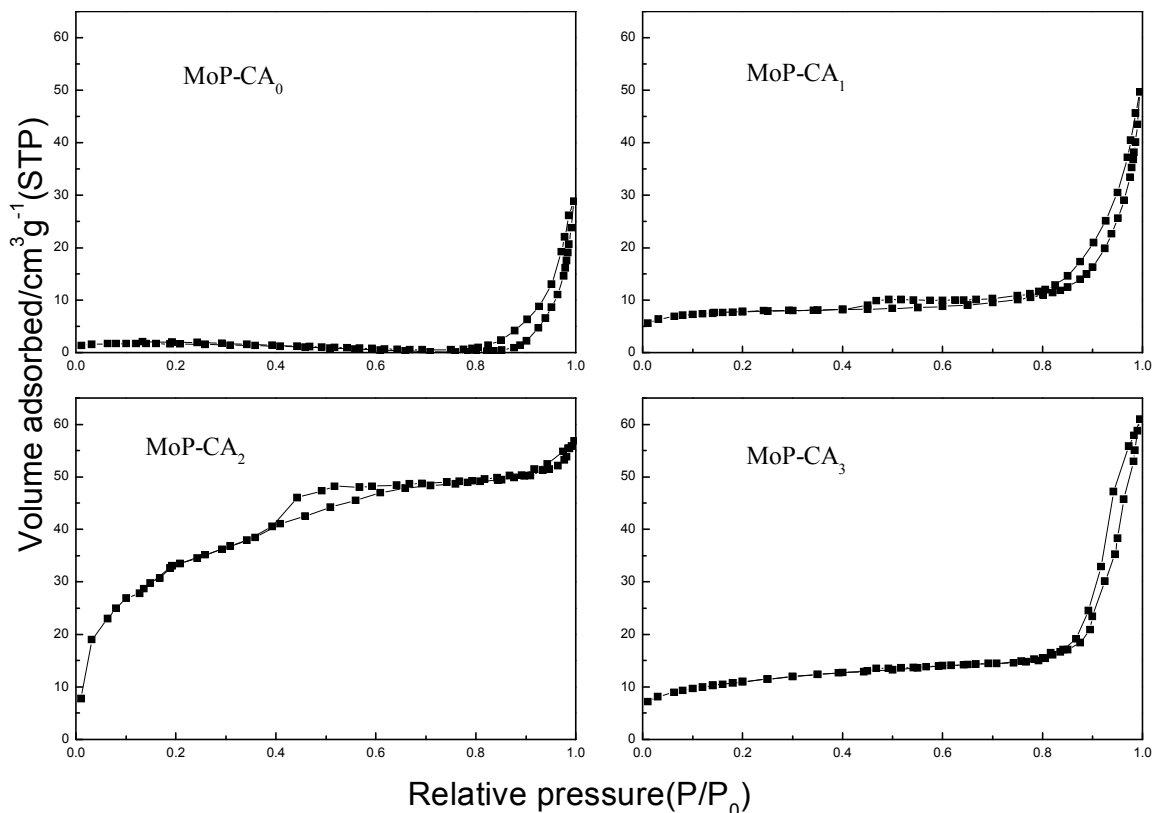


Fig. 1: N₂ adsorption-desorption isotherms of MoP-CA_x (x equals the molar ratio of CA to MoP).

The XRD patterns of different MoP samples are presented in Fig. 2, which are consistent with the literature data [19]. As seen from Fig. 2, the strongest characteristic peak appears at $2\theta = 43.1^\circ$, which is assigned to MoP(101) crystal planes. Other peaks of active phase MoP are at $2\theta = 27.9^\circ, 32.1^\circ, 57.1^\circ,$ and 67.5° , which can be indexed as (001), (100), (110) and (102) of MoP crystal planes, respectively. No impurity peak was detected in the MoP prepared by the combined CA_x-TPR method, suggesting that a pure crystalline compound was formed. It is noted that varying the CA/MoP molar ratios from 0 to 2 slightly changed the average crystallite size from 18.2 to 8.6 nm (calculated from the XRD pattern by the Scherrer equation). However, as the amount of CA continues to increase, the crystallite size will gradually increase. The crystallinity of the MoP-CA_x ($x=0,1,2,3$) samples were 92.75%, 53.15%, 12.44% and about 2%, respectively, which were calculated from the XRD patterns by the soft of Jade5.0. With the increase of x , the crystallinity of the prepared samples sharply declined. So addition of CA does not change the structure of MoP, but it favors to form catalyst particles with smaller size and lower crystallinity.

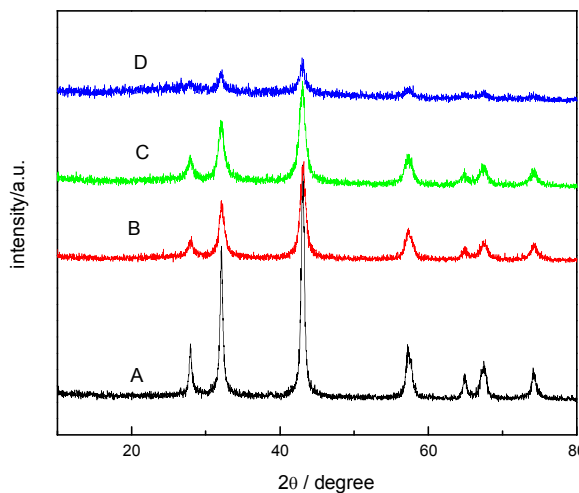


Fig. 2: XRD spectra of MoP-CA₀(A), MoP-CA₁(B), MoP-CA₂(C) and MoP-CA₃(D).

The CO₂-TPD curves of different MoP samples are presented in Fig. 3. As shown in Fig. 3, there are three desorption peaks in TPD curves. The peak (α -CO₂) at low temperature (less than 400K) is physical desorption peak of carbon dioxide, the peak

(β -CO₂) at moderate temperature(500-650K) is desorption peak of CO₂ adsorbed on the weak Lewis basic sites, while the peak (γ -CO₂) at high temperature is desorption peak of CO₂ adsorbed on the strong Lewis basic sites. The peak temperatures(T_p) and areas (A) of CO₂-TPD on the MoP-CA_x catalysts are listed in Table-2. With the addition of CA, the areas of β -CO₂ peak are only slightly increased, while the areas of γ -CO₂ peak significantly increased. This means the existence of CA during the catalyst preparation will lead a significant increase in the number of strong Lewis basic active centers, which is advantageous to DRM reaction [20].

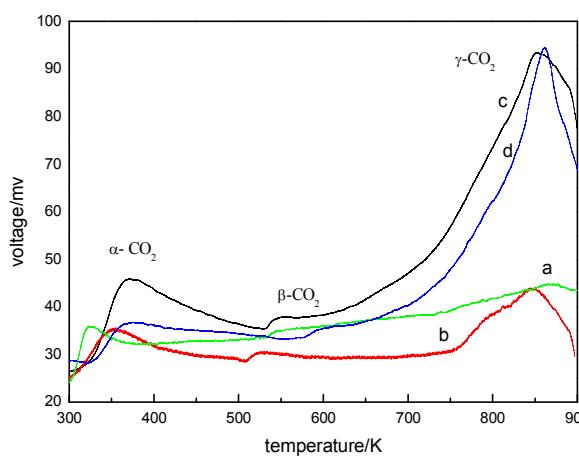


Fig. 3: CO₂-TPD patterns of catalysts MoP-CA₀(a), MoP-CA₁(b), MoP-CA₂(c) and MoP-CA₃(d).

Table- 2: Peak temperature (T_p) and areas (A) of CO₂-TPD on the MoP-CA_x catalysts.

Samples	T_p /K			A		
	α -CO ₂	β -CO ₂	γ -CO ₂	α -CO ₂	β -CO ₂	γ -CO ₂
MoP-CA ₀	325	549	867	3230	1502	2315
MoP-CA ₁	353	529	847	4936	2156	7029
MoP-CA ₂	367	548	851	8372	2645	14542
MoP-CA ₃	372	608	860	4442	2509	12744

Effects of CA Addition on the Catalytic Activity of Molybdenum Phosphide Catalysts

Table-3 lists the results of activities for different catalysts. With the increase of x , the initial activity of DRM reaction increased firstly and then decreased, the highest catalytic activity was observed in the sample with $x = 1$. This can be interpreted as follows. Firstly, addition of suitable CA could increase the special surface areas of catalysts, reduce the catalysts particles size and improve the dispersion of MoP active particles. Thus, the initial catalytic activity of MoP-CA₁ and MoP-CA₂ for DRM reaction

increased. For MoP-CA₃, more CA could be aggregated as template to form the cluster of the MoP particles, which reduce the dispersion of MoP active particles and decrease the catalytic activity. Secondly, addition of CA results in the increased amount of adsorbed CO₂ and in a shift of the γ -CO₂ desorption peak to lower temperature, which means more active centers of strong Lewis basic could be formed by the catalysts prepared with CA. These catalysts can promote adsorption and dissociation of carbon dioxide, because CO₂ is an acidic gas. In the meantime, carbon deposition is suppressed with strong Lewis basicity of the surface [21], which in turn promoted the activity of catalysts. In addition, the adsorption of CH₄ can be hindered for the competitive adsorption with CO₂. The γ -CO₂ desorption at high temperature was important to DRM reaction, the T_p of MoP-CA₁ was the lowest among these catalysts, which was advantageous to the dissociation of carbon dioxide and the competitive adsorption between CH₄ and CO₂ [8]. Therefore, the catalytic activity of MoP-CA₁ was the highest and active temperature range was the widest, which was in accordance with experimental results.

Table-3: The conversion efficiency with selected catalysts at different temperatures.

Sample	Reaction temperature (K)	Conversion (%)		Resultants(%)			
		X(CH ₄)	X(CO ₂)	CH ₄	CO ₂	CO	H ₂
MoP-CA ₀	973	43.64	66.33	30.22	15.62	36.93	17.24
	1023	59.78	60.61	21.57	18.27	38.34	21.82
	1073	70.31	80.54	15.92	9.03	45.15	29.91
MoP-CA ₁	973	52.27	91.33	26.18	3.91	52.60	17.30
	1023	75.70	90.16	13.33	4.44	47.54	34.69
	1073	85.07	95.44	8.19	2.06	49.50	40.25
MoP-CA ₂	973	55.01	67.81	24.13	14.93	43.08	17.87
	1023	65.43	84.63	18.54	7.13	45.57	28.76
	1073	72.78	90.34	14.59	4.48	47.76	33.16
MoP-CA ₃	973	42.82	67.06	30.66	15.28	35.72	18.34
	1023	52.90	84.17	25.26	7.34	56.23	11.17
	1073	66.19	76.52	18.13	10.66	54.42	16.56

The Samples Prepared with CA had Good Anti-Sintering Ability, Stability and Reproducibility.

Fig. 4 showed the time course of the DRM reaction at 1023K for MoP catalysts. The result showed that MoP catalysts prepared with CA exhibited higher stability. MoP-CA₁ showed a very high stability during the whole reaction time. MoP-CA₂ showed a slight decrease in CH₄ conversion. The lowest stability was observed for the MoP-CA₀ catalyst prepared without CA. This catalyst showed a high degree of deactivation, especially during 2h of reaction.

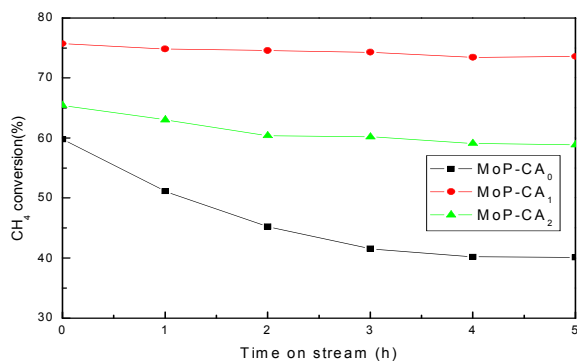


Fig. 4: CH₄ conversion over MoP-CA₀, MoP-CA₁, and MoP-CA₂ catalysts during the time course of CH₄-CO₂ reforming reaction. ($V(\text{CH}_4)/V(\text{CO}_2)=1$; 0.1 MPa; 1023 K; SV: 2000 mL/(g-cat·h).)

The catalyst structure was completely stable to the reaction conditions. Fig. 5 showed the XRD patterns of the MoP-CA₁. After continuous reaction at 1023 K for 5h, no extra diffraction peaks appeared except the characteristic peaks of molybdenum phosphide (Fig. 5C). When the post-reaction catalysts were reduced in H₂ flow (60 ml/min) at 923 K for 2 hours, MoP crystals were obtained again (Fig. 5D). The average methane conversion yields by MoP-CA₁ and reduced post-reaction MoP-CA₁ were 75.7% and 75.51%, respectively. The catalytic activity of the regenerated catalyst did not change significantly.

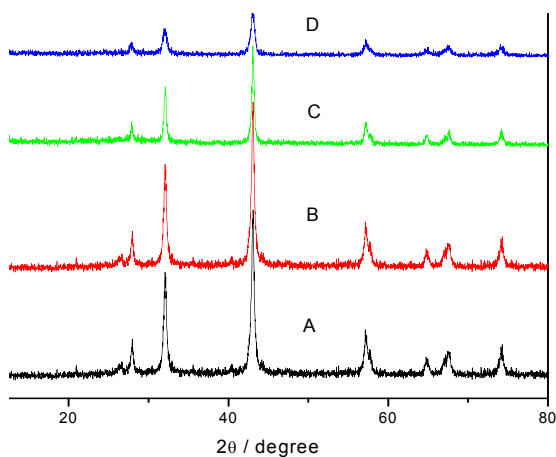


Fig. 5: XRD patterns of MoP-CA₁: (A) precursor calcined at 773K, (B) reduced at 923K, (C) continuous reaction at 1023K for 5h and (D) reduced at 923K after continuous reaction for 5h

Conclusion

The addition of citric acid can improve the physical structure properties of MoP catalysts, but can not change the crystal phase structure properties of MoP. These catalysts have good activities towards methane dry reforming with CO₂. Among all the catalyst formulations studied by us, the activity of MoP-CA₁ is the highest with the widest active temperature range. In higher temperatures, the MoP-CA₁ catalyst exhibit good anti-sintering ability and high stability. After reduced in H₂ flow at 923 K, the activity of the post-reaction catalyst can be well restored, while its structure remains unchanged.

Acknowledgements

Financial support from the National Natural Science Foundation of China (21063010) is gratefully appreciated.

References

1. P. Ferreira-Aparicio, M. J. Benito and J. L. Sanz, New Trends in Reforming Technologies: from Hydrogen Industrial Plants to Multifuel Microreformers, *Catal. Rev.*, **47**, 491 (2005).
2. H. Martin, How Stable Is the Methane Cycle? *Sci.*, **327**, 1211 (2010).
3. S. Barama, C. D. Batiot, M. Capron, E. Bordes-Richard, O. B. Mohammedi, Catalytic Properties of Rh, Ni, Pd and Ce Supported on Al-pillared Montmorillonites in Dry Reforming of Methane, *Catal. Today*, **141**, 385 (2009).
4. M. Nagai, K. Nakahira, Y. Ozawa, Y. Namiki, Y. Suzuki, CO₂ Reforming of Methane on Rh/Al₂O₃ Catalyst, *Chem. Eng. Sci.*, **62**, 4998 (2007).
5. J. R. Mawdsley, T. R. Krause, Rare Earth-First-Row Transition Metal Perovskites as Catalysts for the Autothermal Reforming of Hydrocarbon Fuels to Generate Hydrogen, *Appl. Catal. A*, **334**, 311 (2008).
6. D. P. Liu, L. Raymond, B. Armando, Y. H. Yang, Carbon Dioxide Reforming of Methane to Synthesis Gas over Ni-MCM-41 Catalysts, *Appl. Catal. A*, **358**, 110 (2009).
7. B. Q. Xu, J. M. Wei, Y. T. Yu, Y. Li, J. L. Li and Q. M. Zhu, Size Limit of Support Particles in an Oxide-Supported Metal Catalyst: Nanocomposite Ni/ZrO₂ for Utilization of Natural Gas, *J. Phys. Chem. B*, **107**, 5203 (2003).
8. X. C. Li, M. Wu, Z. H. Lai and F. He, Studies on Nickel-Based Catalysts for Carbon Dioxide

- Reforming of Methane, *Appl. Catal. A*, **290**, 81 (2005).
- X. C. Li, S. G. Li, Y. F. Yang, M. Wu and F. He, Studies on Coke Species of Nickel-Based Catalysts in CO₂ Reforming of CH₄, *Catal. Lett.*, **118**, 59 (2007).
 - B. Steinhauer, M. R. Kasireddy, J. Radnik and A. Martin, Development of Ni-Pd Bimetallic Catalysts for the Utilization of Carbon Dioxide and Methane by Dry Reforming, *Appl. Catal. A*, **366**, 333 (2009).
 - S. T. Oyama, Novel Catalysts for Advanced Hydroprocessing: Transition Metal Phosphides, *J. Catal.*, **216**, 343 (2003).
 - J. Gopalakrishnan, S. Pandey, K. K. Rangan, Convenient Route for the Synthesis of Transition Metal Pnictides by Direct Reduction of Phosphate, Arsenate, and Antimonite Precursors, *Chem. Mater.*, **9**, 2113 (1997).
 - W. Li, B. Dhandapani, S. T. Oyama, Molybdenum Phosphide: A Novel Catalyst for Hydrodenitrogenation, *Chem. Lett.*, **27**, 207 (1998).
 - C. Stinner, R. Prins, T. Weber, Binary and Ternary Transition-Metal Phosphides as HDN Catalysts, *J. Catal.*, **202**, 187 (2001).
 - P. Clark, W. Li and S. T. Oyama, Synthesis and Activity of a New Catalyst for Hydroprocessing: Tungsten Phosphide, *J. Catal.*, **200**, 140 (2001).
 - F. X. Sun, W. C. Wu, Z. L. Wu, J. Guo, Z. B. Wei, Y. X. Yang, Z. X. Jiang, F. P. Tian, C. Li, Dibenzothiophene Hydrodesulfurization Activity and Surface Sites of Silica-Supported MoP, Ni₂P, and NiMoP Catalysts, *J. Catal.*, **228**, 298 (2004).
 - Y. Teng, A. J. Wang, X. Li, J. G. Xie, Y. Wang, Y. K. Hu, Preparation of High-Performance MoP Hydrodesulfurization Catalysts via a Sulfidation-Reduction Procedure, *J. Catal.*, **266**, 369 (2009).
 - R. H. Cheng, Y. Y. Shu, L. Li, M. Y. Zheng, X. D. Wang, A. Q. Wang and T. Zhang, Synthesis and Characterization of High Surface Area Molybdenum Phosphide, *Appl. Catal. A*, **316**, 160 (2007).
 - S. Rundqvist, T. Lundstrom, X-Ray Studies of Molybdenum and Tungsten Phosphides, *Acta Chem. Scand.*, **17**, 37 (1963).
 - C. L. Li, Y. L. Fu and G. Z. Bian, Surface Basicity and Catalytic Performance on Ni/Ce-Zr-Al-O Catalyst for CO₂+CH₄ Reforming, *Acta Phys.-Chim. Sin.*, **19**, 902 (2003).
 - T. Horiuchi, K. Sakuma, T. Fukui, Y. Kubo, T. Osaki and T. Mori, Suppression of Carbon Deposition in the CO₂-Reforming of CH₄ by Adding Basic Metal Oxides to a Ni/Al₂O₃ Catalyst, *Appl. Catal. A*, **144**, 111 (1996).